Short-Term Regulation of Excitation-Contraction Coupling by the β_{1a} Subunit in Adult Mouse Skeletal Muscle

María C. García,* Elba Carrillo,* José M. Galindo,* Ascensión Hernández,* Julio A. Copello,† Michael Fill,‡ and Jorge A. Sánchez*

*Departmento de Farmacología, Centro de Investigación y de Estudios Avanzados del I.P.N., Mexico, D.F. 07360, Mexico; †Department of Pharmacology, Southern Illinois University, Springfield, Illinois; and ‡Department of Physiology, Loyola University Chicago, Maywood, Illinois

ABSTRACT The β_{1a} subunit of the skeletal muscle voltage-gated Ca^{2+} channel plays a fundamental role in the targeting of the channel to the tubular system as well as in channel function. To determine whether this cytosolic auxiliary subunit is also a regulatory protein of Ca^{2+} release from the sarcoplasmic reticulum in vivo, we pressure-injected the β_{1a} subunit into intact adult mouse muscle fibers and recorded, with Fluo-3 AM, the intracellular Ca^{2+} signal induced by the action potential. We found that the β_{1a} subunit significantly increased, within minutes, the amplitude of Ca^{2+} release without major changes in its time course. β_{1a} subunits with the carboxy-terminus region deleted did not show an effect on Ca^{2+} release. The possibility that potentiation of Ca^{2+} release is due to a direct interaction between the β_{1a} subunit and the ryanodine receptor was ruled out by bilayer experiments of RyR1 single-channel currents and also by Ca^{2+} flux experiments. Our data suggest that the β_{1a} subunit is capable of regulating E-C coupling in the short term and that the integrity of the carboxy-terminus region is essential for its modulatory effect.

INTRODUCTION

Dihydropyridine receptors (DHP) play an essential role as the voltage sensors that link excitation with contraction in skeletal muscle (for reviews, see Ríos and Pizarro and others 1–4). In addition to their role as voltage sensors, these receptors are also permeant to Ca^{2+}, generating a very slowly activated L-type Ca^{2+} current ((5) for a review, see Melzer et al. (4)). DHP receptors are composed of the main subunit $\alpha_{1s,}$ and the auxiliary subunits, α_2-δ, β_1, and γ-subunits. The α_{1s} subunit (now referred to as the $Ca_V1.1$ channel (6)) contains the pore (7), the voltage sensor of excitation-contraction coupling, and the DHP binding sites (for reviews, see Ríos and Pizarro and others (1,8–10)).

The β_{1a} subunit is the main isoform among the β_1 subunits present in skeletal muscle (11) and its role has been explored by inactivating the β_1 gene using gene targeting techniques. This approach has revealed that this subunit plays an essential role in the assembly of DHP receptors in their correct position. β-null cells have undetectable levels of the α_{1s} subunit in the cell membrane and show greatly reduced L-type Ca^{2+} currents and charge movement (12,13), an effect that can be reversed by the introduction of the cDNA of the β_{1a} subunit (14). However, much less is known about the potential role of this auxiliary subunit as a modulatory protein of E-C coupling, regulating Ca^{2+} release in the short term. In this regard, we have recently described that the addition of the β_{1a} subunit to a cell-free preparation enhances the amplitude of L-type current within minutes, consistent with a short-term modulatory role on $Ca_V1.1$ channels (15). The aim of this study was to examine whether the β_{1a} subunit also has a short-term effect on Ca^{2+} release induced by action potentials in adult skeletal muscle fibers.

Preliminary results have been published (16).

MATERIALS AND METHODS

Fiber preparation

BALB/c mice (aged ~9 weeks) were used. These were killed by cervical dislocation, after which the flexor digitorum brevis muscles (FDB) of the hindlimbs were isolated and incubated at 34°C for 60 min in a Ca^{2+}-Mg^{2+}-free Tyrode solution plus 10% fetal calf serum (Gibco-Invitrogen, Carlsbad, CA) and collagenase (0.5 mg/ml, type lV, Sigma, St. Louis, MO). The muscles were then rinsed and dissociated by gently triturating the enzyme-treated muscles through a fire-polished Pasteur pipette with collagenase-free Tyrode solution containing (mM): NaCl, 146; KCl, 5; $CaCl_2$, 2; $MgCl_2$, 1; glucose, 11; HEPES, 10; at pH = 7.4. The experiments were performed according to the guidelines of the local animal care committee.

Molecular biology techniques

Production of the β_{1a} subunit in COS-1 cells

We have described the expression and detailed purification procedure of the β_{1a} subunit in COS-1 cells elsewhere (15). In brief, COS-1 cells were transiently transfected with a plasmid containing the cDNA of the β_{1a} subunit (pSG5-Mβ_{1a}) under the control of the SV-40 promoter. Membrane fraction samples of homogeneized COS-1 cells were loaded onto polyacrylamide gels and stained with Coomassie blue. The gel band that contained the β_{1a} subunit was identified by Western blots, cut, and purified by electroelution methods according to Smith (17). After the electroelution procedure, electrodialysis techniques were used to remove all traces of sodium dodecyl sulfate, as described by García et al. (15). The dried protein was stored at −20°C until used.

Submitted May 23, 2005, and accepted for publication September 13, 2005.

Address reprint requests to Dr. Jorge A. Sánchez, Dept. of Pharmacology, Cinvestav Apartado Postal 14-740, Mexico, D.F. 07360. Tel.: 52-55-5061-3301; Fax: 52-55-5577-7090; E-mail: jsanchez@cinvestav.mx.

0006-3495/05/12/3976/09 $2.00

doi: 10.1529/biophysj.105.067116

Bacterial production and purification of the β_{1a} subunit

The coding fragment of the β_{1a} subunit was liberated from the pSG5 expression vector mentioned above. To this end, pSG5-β_{1a} was cleaved with *Nhe*I (New England Biolabs, Beverly, MA). *Nhe*I sites are present in both ends of the β_{1a} fragment. The sticky ends of the fragment were filled with Klenow polymerase and ligated at the *Sma*I site of the multiple cloning site of the pQE-31 vector (Qiagen, Valencia, CA). This strategy generates an in-frame cloning of the β_{1a} protein. *Escherichia coli* DH5-α cells were transformed with this construct and clones with the correct orientation of the insert were selected to achieve transcription of the product with the T5 promoter present in the vector. The deletion of the last 40 amino acids in the carboxy-terminus region of the β_{1a} subunit was achieved by cleavage of pSG5-β_{1a} plasmid with *Not*I. The plasmid contains a single recognition site located downstream from the open reading frame. After that, DNA was treated with *Bal*-31 exonuclease (New England Biolabs) for 15 min. To estimate the size of the deleted products, we used *Nco*I and *Hinc*II to liberate the 3′ end of the β_{1a} subunit and the products were subsequently sequenced. The fragment containing the truncated β_{1a} was liberated from the pSG5 vector by *Nhe*I and *Hinc*II (New England Biolabs). It was then filled with Klenow polymerase and subcloned in the same way as the nontruncated β_{1a} subunit. Both clones were sequenced to confirm the integrity of the open reading frame with Sequenase kit (version 2.0, USB) and specific oligonucleotides for pQE vectors. Deletion of 40 amino acids in the C-terminus region of the β-subunit is not expected to alter the folding of the protein. In fact, Bogdanov et al. (18) produced chimeras of β-subunits lacking more amino acids in their C-terminus region than in this study and suggested that no disruption in protein folding takes place. In addition, molecular models of β-subunits have identified several domains that allow intramolecular interactions, namely, SH3 domain, PDZ domain, and the GK domain (19,20). None of these domains is located in the C-terminus region of the β-protein and the domain organization of D2 and D4 domains is not altered by a similar C-terminus deletion (21).

E. coli BL21(λDE3) (Novagen, San Diego, CA) cells were transformed with the above constructs and used for mass production of the β_{1a} subunit protein and its truncated form. The cells were cultured in 100 ml of LB medium in the presence of 100 μg/ml ampicillin and grown at 32°C until an A_{600} of 0.6 was reached. The production of the protein was induced by 1.0 mM isopropyl β-D-thiogalactopyranoside for 6 h at 32°C. The cells were pelleted and resuspended in 10 ml of NETN buffer (NaCl = 120 mM, Tris-HCl = 20 mM, EDTA = 1 mM, PSMF = 1 mM, and 0.5% NP-40 at pH = 8.0). Cell lysis was achieved with the aid of a French press (Thermo Spectronic, Shelton, CT) at a pressure of 600 psi, applied twice. The lysate was centrifuged at 15,000 × *g* resulting in a pellet and in a clear supernatant fraction. The β_{1a} subunit protein was found in the pellet fraction and was solubilized with 5 M urea. The truncated form of the β_{1a} subunit was found in the supernatant. The protein fractions were analyzed by SDS-PAGE and stained with Coomassie blue. The β_{1a} subunit was identified by Western blot as described elsewhere (15). The products were obtained by electroelution techniques and the eluted protein products were precipitated with acetone. Thereafter, the samples were dialyzed with water to remove the salt content.

Pressure injection techniques

To introduce the β_{1a} subunit into muscle fibers, we used an intracellular micropipette to which pressure was applied. The micropipettes were pulled in a Brown-Flaming horizontal puller (Sutter Instruments, San Francisco, CA) from Kwik-fill glass capillaries (WPI, New Haven, CT) and had an average resistance of 25 MΩ when filled with 3 M KCl. They were mounted in a plastic holder and driven by a hydraulic micromanipulator (Narishige MO-150, Tokyo, Japan). Pipettes were filled with a solution containing (mM): KCl, 140; $MgCl_2$, 1; EGTA, 1; and HEPES, 10, at pH = 7.1. Fibers were impaled at a point located 125 μm from the position where light was detected with the photodiode. The β_{1a} subunit, purified either from COS-1 cells or from bacteria, was used at a concentration of 0.35 μg/μl. Most experiments were performed with β_{1a} subunits purified from COS-1 cells. Experiments that were performed with β_{1a} subunits from bacteria are clearly indicated in the text. Control experiments involved pressure injection of a heat-inactivated β_{1a} subunit added at the same concentration or pressure injection of the micropipette saline solution. In both cases, these control injections gave similar results and are considered together in the Results section. Two trains of pulses separated by a 30-s interval were delivered. Each train consisted of five consecutive 150 kPa pressure pulses, each lasting 600 ms. We estimate that this procedure allowed the injection of 40–50 pl of solution. Action potentials were elicited by passing rectangular current pulses between two platinum plate electrodes placed symmetrically on either side of the muscle chamber.

The microinjected β_{1a} subunit is expected to diffuse away from the point of injection along the axis of the muscle fiber. To estimate the diffusion of the β_{1a} subunit in our experiments, we used Fick's second law (Eq. 1). This equation was used by Papadopoulos et al. (22) to account for the axial spread of microinjected proteins in muscle. In Eq. 1, D is the diffusion coefficient and C is the concentration of the injected protein in the sarcoplasm that changes as a function of time (t) and as a function of the distance from the point of injection (x). Equation 1 describes the proportionality between the change of C along the diffusion pathway $\partial C/\partial x$ and the change in concentration with time $\partial C/\partial T$. This equation assumes a one-dimensional diffusion process with an infinite extension of the diffusion path.

$$\delta C/\delta t = D \times \delta^2 C/\delta x^2. \quad (1)$$

The diffusion coefficient (D) in Eq. 1 was measured experimentally in the myoplasm of muscle fibers by Papadopoulos et al. (22) for proteins of different masses. In our estimations we used $D = 6.2 \times 10^{-8}$ cm^2 s^{-1}. This value corresponds to the diffusion coefficient measured for hemoglobin (22), a protein that has a similar mass (64.5 kDa) to that of the β_{1a} subunit (55 kDa (10)). The analytical solution of Eq. 1 can be achieved using a Dirac delta function applied at $t = 0$. The solution is Eq. 2 where A is an amplitude factor.

$$C = A(4\pi Dt)^{-1/2} \times \exp[(-x^2)/4Dt]. \quad (2)$$

Optical techniques

We used Fluo-3 AM (1–10 μM) (Molecular Probes, Eugene, OR) to monitor the levels of intracellular Ca^{2+}. This dye undergoes large fluorescence changes upon Ca^{2+} binding, it has a large dynamic range, low compartmentalization (23), and it has been used extensively in muscle (24–26). Fibers were mounted in a chamber placed on the stage of an Optiphot microscope (Nikon, Tokyo, Japan). The fluorescence emitted by a preselected region of a stained muscle fiber, illuminated episcopically with monochromatic light at a wavelength of 485 nm, was filtered with a high-pass barrier filter (cut-on wavelength 535 nm), and detected with a low noise photodiode connected in a photovoltaic configuration. The basal fluorescence (F) from the same region of the muscle fiber was recorded continuously on video tape. Its mean value during 300 ms before electrical stimulation, was used to scale Ca^{2+} signals as $\Delta F/F$. This procedure minimizes the possible effects of changes in the concentration of the dye on fluorescence signals and it has been used extensively by others (24,27). No attempts were made to calculate the actual myoplasmic Ca^{2+} concentration. To prevent mechanical artifacts, intact single fibers were suspended in 0.35% agar gel, following a procedure similar to that described in (28) except that we used a lower agar concentration and that our experiments were performed at a lower temperature (20–22°C).

Ca^{2+} leak measurements

Skeletal muscle heavy sarcoplasmic reticulum (SR) microsomes were obtained following procedures by Saito et al. (29). The net rate of Ca^{2+} leak from these microsomes was measured at room temperature (20–24°C) with

a spectrophotometer (Cory 50, Varian, Palo Alto, CA) using the Ca^{2+}-sensitive dye antipyrylazo III (APIII). Changes in Ca^{2+} concentration over time were measured as the absorbance difference between 710 and 790 nm as described in (30). Briefly, microsomes (50 μg protein) were incubated with 1 ml of assay solution containing 100 mM potassium phosphate, 0.2 mM APIII, 4 mM $MgCl_2$, and 2 mM ATP (pH 7). Microsomes were actively preloaded with Ca^{2+} (via the SR Ca^{2+} ATPase) by adding 3 aliquots of 40 nM $CaCl_2$ while stirring. The microsomes were then incubated for 5 min with standard buffer (control) or buffer containing ruthenium red (5 μM), normal β_{1a} subunit, or the truncated β_{1a} subunit. After this incubation period, 25 μM cyclopiazonic acid (CPZ) was added to inhibit the SR Ca^{2+} ATPase and then Ca^{2+} leak from the microsomes was monitored. When caffeine (2.5 mM) was applied, it was applied simultaneously with CPZ. Ca^{2+} leak rate in each experimental condition was measured from the slope of the APIII Ca^{2+} signal.

Electrophysiological methods

Dissociated FDB muscle fibers were used in voltage clamp experiments. To minimize mechanical artifacts during measurements of membrane currents, fibers were not embedded in agar as in optical experiments. Instead, movement artifacts were greatly suppressed by a previous incubation for 3 h in the cell permeant calcium buffer BAPTA AM (10 mM) (Molecular Probes).

The whole-cell patch-clamp technique was used to record $Ca_V1.1$ currents (31). Pipettes (1–1.2 MΩ) were double-pulled from hard glass (KIMAX-51; Kimble Glass, Toledo, OH) and were filled with 5 μl of the internal solution. $Ca_V1.1$ currents were measured 10 min after achieving the whole cell configuration. The β_{1a} subunit was tested by adding 0.30–0.35 μg μl^{-1} of the β_{1a} subunit to the pipette solution. Currents were recorded with an Axopatch 200A (Axon Instruments, Foster City, CA) amplifier; 60–80% of the series resistance was electronically compensated.

To measure charge movement, command pulses of 60-ms duration and variable amplitude were delivered. The pulse sequence was bracketed by 16 consecutive hyperpolarizing control pulses, −20 mV from the holding potential (E_h) that was set at −100 mV. The currents generated during these pulses were used to subtract linear membrane components, to calculate the linear membrane capacitance, and to measure the leakage current during the experiment.

The voltage dependence of activation of nonlinear charge movement was fitted to the Boltzmann function:

$$Q = Q_{max}/\{1 + \exp[(V - V_m)/k]\}, \quad (3)$$

where Q_{max} is the maximum value of charge, V_m is the membrane potential, V is the potential where $Q = 0.5\ Q_{max}$, and k is a measure of the steepness of the curve.

To measure Ca^{2+} currents (I_{Ca}) the same pulse protocol was used except that the duration of the pulses was 750 ms and $E_h = -80$ mV. The interval between pulses was 4 s. The peak Ca^{2+} current values were fitted to Eq. 4, which is similar to that used by Wang et al. (32) to describe the current-voltage relationship of L-type Ca^{2+} currents in muscle fibers.

$$I_m = G_{max} \times (V_m - V_{rev})/\{1 + \exp[V - V_m)/k]\}. \quad (4)$$

In Eq. 4, G_{max} is the maximum conductance and V_{rev} is the reversal potential. The other parameters have the same meaning as in Eq. 3.

Single channel measurements of skeletal RyR1 channels were recorded by fusing SR microsomes into artificial planar lipid bilayers as previously described by Copello et al. (33). Briefly, planar bilayers were formed by painting a mixture (5:4:1) of phosphatydilethanolamine, phosphatydilserine, and phosphatydilcholine (50 mg/ml decane) across a 100-μm hole separating two ~1-ml solutions. One solution (*trans*) contained 250 mM HEPES/50 mM $Ca(OH)_2$ (pH 7.4) and was clamped to 0 mV using an Axopatch 200B patch-clamp amplifier (Axon Instruments). The other solution (*cis*) was held at virtual ground and contained 1 mM CsCl, 250 mM HEPES/Tris (pH 7.4), and 1 mM $CaCl_2$. The SR microsomes (5 μg protein) were added to the *cis* solution while stirring. In this situation, the RyR1 channels incorporate with their cytosolic surface facing the *cis* solution. Channels were identified by their high conductance, Ca^{2+} selectivity, and gating characteristics. After RyR1 incorporation, the *cis* solution was perfused with 30 vol of 250 mM HEPES/Tris (pH 7.4) and the free Ca^{2+} level was adjusted to ~2 μM (1.4 mM $CaCl_2$, 1 mM BAPTA, and 1 mM DiBromoBAPTA). The *cis* solution also contained 7 mM ATP and 5.5 mM Mg^{2+}. Single-channel recordings were made before and after addition of β_{1a} subunit (1–4 μM; stirring for 2 min) to the *cis* solution. Recordings were filtered at 1000 Hz and digitized at 20 KHz with a Digidata 1360 acquisition system (Axon Instruments). Data were analyzed using pClamp9 (Axon Instruments). Open probability (*Po*) was determined from at least 8 min of recording.

Electrophysiological and optical experiments were carried out at room temperature (20–22°C).

Solutions

The external solution employed to record I_{Ca} contained (mM): 10 Ca^{2+}, 140 $TEACH_3SO_3$ (tetraethylamonium methanesulphonate), and 2 $MgCl_2$. The pipette solution contained (mM): 140 Cs-aspartate, 5 $MgCl_2$, and 10 EGTA. The composition of the external solution used to record charge movement was similar, except that the concentration of external Ca^{2+} was reduced to 1 mM. The presence of Ca^{2+} was required to maintain the stability of our recordings because fibers do not generally tolerate the absence of Ca^{2+} well. We did not use Ca^{2+} channel blockers because they alter the voltage dependence of charge movement and may have deleterious effects on leakage currents (34). Due to the contamination of ''off'' charge by tail Ca^{2+} currents, we restricted our measurements to ''on'' charge only. Contamination of ''on'' charge by I_{Ca} is likely to be minor because charge moves at more negative potentials than I_{Ca} and the time course of activation of I_{Ca} is very slow compared to that of ''on'' charge (32). In fact, it has been shown that integration of ''on'' charge provides an accurate measure of charge movement in Ca^{2+}-contaning solutions, even without Ca^{2+} channel blockers (35).

Extracellular and intracellular solutions were buffered with HEPES (10 mM) at pH 7.2 and 7.1, respectively. Chemicals were obtained from either Sigma Chemical or Aldrich Chemical (St. Louis, MO).

The fitting of numerical formulas to experimental data employed a nonlinear, least squares algorithm. Parameter values given in the text are expressed as mean ± SE. Student's *t*-test was used at the level $p < 0.05$ to calculate statistical significance of the data.

RESULTS

Actions of the β_{1a} subunit on intracellular Ca^{2+} signals

Fig. 1 *A* shows Ca^{2+} transients from a control experiment recorded from a single FDB skeletal muscle fiber. The recorded region was located ~125 μm from the point of injection. Illustrated are Ca^{2+} signals recorded before and after the injection of a control solution (at $t = 0$). The change in fluorescence of the dye is expressed as a $\Delta F/F$ ratio. The transient increase in Fluo-3 fluorescence induced by an action potential rapidly reaches a peak and decays quickly initially and then, more slowly to prestimulus levels. The fiber was stimulated extracellularly at the times indicated (in minutes) by the numbers above each trace. The Ca^{2+} transients were quite similar before and after pressure injection indicating that the injection, by itself, had only minor effects on Ca^{2+} release. A very different result was observed when the β_{1a} subunit was

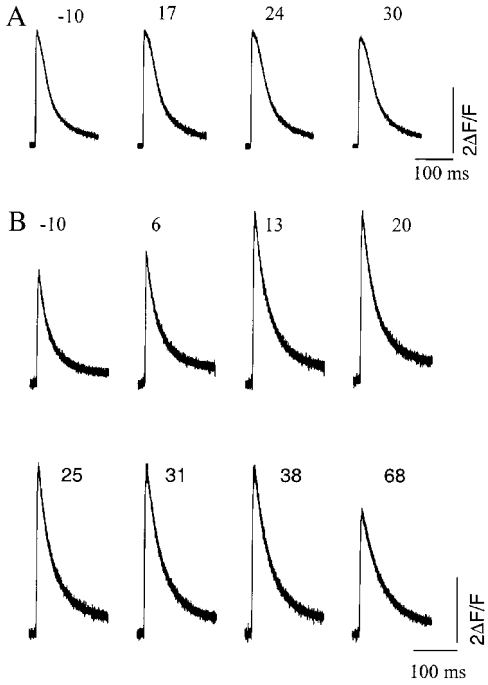

FIGURE 1 The action of the β_{1a} subunit upon Ca signals. (*A*) The records show Fluo-3 Ca^{2+} signals associated with action potentials from a muscle fiber that was pressure injected with a control solution. (*B*) Ca^{2+} signals from a separate fiber to which the β_{1a} subunit was pressure injected. The numbers below each trace indicate time in minutes computed since microinjection was done.

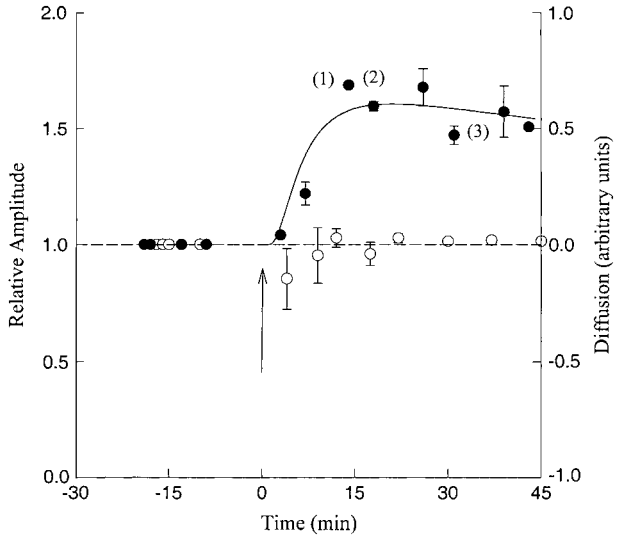

FIGURE 2 The time course of action of the β_{1a} subunit. Circles represent mean values (± SE) of peak Ca^{2+} signals as a function of time. Values were normalized for every experiment as: Peak *j* / Peak *a*, where *j* is every individual peak Ca^{2+} signal value and *a* is the average peak value of signals recorded before pressure injection; (○) represents values of normalized records obtained from pressure-injected fibers with the control solution; (●) represents values from pressure-injected fibers with the β_{1a} subunit. The arrow indicates time of microinjection. Unless otherwise indicated by the number in parentheses, each symbol represents the mean value of at least five to seven separate experiments. The smooth curve is the graph of Eq. 2 at $x = 125$ μm and $D = 6.2 \times 10^{-8}$ cm^2 s^{-1}.

injected. The β_{1a} subunit had remarkable effects on Ca^{2+} signals generated by action potentials (Fig. 1 *B*). The amplitude of the Ca^{2+} transients increased and this potentiation was evident a few minutes after the β_{1a} subunit was pressure injected. The potentiation reached a peak ~20 min after the injection and then slowly declined to preinjection values. The time course of β_{1a} subunit action is summarized in Fig. 2. To compare data from different experiments, the ratio between the peak amplitude of the Ca^{2+} signal, at any given time, relative to its mean value before pressure injection, was computed for every experiment. Their average values are shown in Fig. 2. Each symbol represents mean values (± SE). Open symbols represent results from fibers that were pressure injected with a control solution. Solid circles represent results from fibers that were pressure injected with the β_{1a} subunit. The smooth curve is the solution of Eq. 2 with the parameters indicated in the legend. It describes rather well the time course of the effect of the β_{1a} subunit on peak $\Delta F/F$ signals. The most significant effect of the β_{1a} subunit was to increase the peak amplitude of the Ca^{2+} transient. There were only minor changes in their time course that were not statistically significant. Before pressure injection of the β_{1a} subunit, the half-time and decay-time constant of the Ca^{2+} transients averaged 42.8 ± 4.9 ($n = 13$) ms and 40.9 ± 4.5 ($n = 13$) ms, respectively. After the injection of the β_{1a} subunit, these parameters were 46.1 ± 4.8 ($n = 13$) ms and 38.6 ± 4.3 ($n = 13$) ms, respectively.

Actions of the β_{1a} subunit on charge movement of muscle fibers

The β_{1a} subunit regulates the amplitude of L-type currents that flow through α_{1s}, the principal subunit of the Ca^{2+} channel in muscle. Because the α_{1s} subunit also generates the charge movement associated with Ca^{2+} release, it is important to determine if the increase in the amplitude of the Ca transient, described above, is associated with similar changes in charge movement.

To measure charge movement, voltage clamp experiments were carried out in FDB muscle fibers. We chose this preparation because of the small fiber size that favors diffusion of the β_{1a} subunit and provides better space clamp than large fibers. The mean fiber length and diameter were 565 ± 26 μm ($n = 12$) and 29 ± 2 μm ($n = 12$), respectively. The mean capacitance was 899 ± 72 pF ($n = 12$). The expected capacitance, assuming a value of 1 μF cm^{-2}, was 508 ± 26 pF ($n = 12$).

Fig. 3 *A* illustrates the relationship between the amount of mobilized charge and membrane potential from control experiments. Each symbol represents average values ± SE. The smooth curve is the best fit of Eq. 3 with the parameters indicated in the legend. The Boltzmann parameters in Fig. 3 *A* are similar to those found by Collet et al. (36) in FDB muscle fibers. The inset shows nonlinear currents from a representative experiment at the potential indicated (in mV)

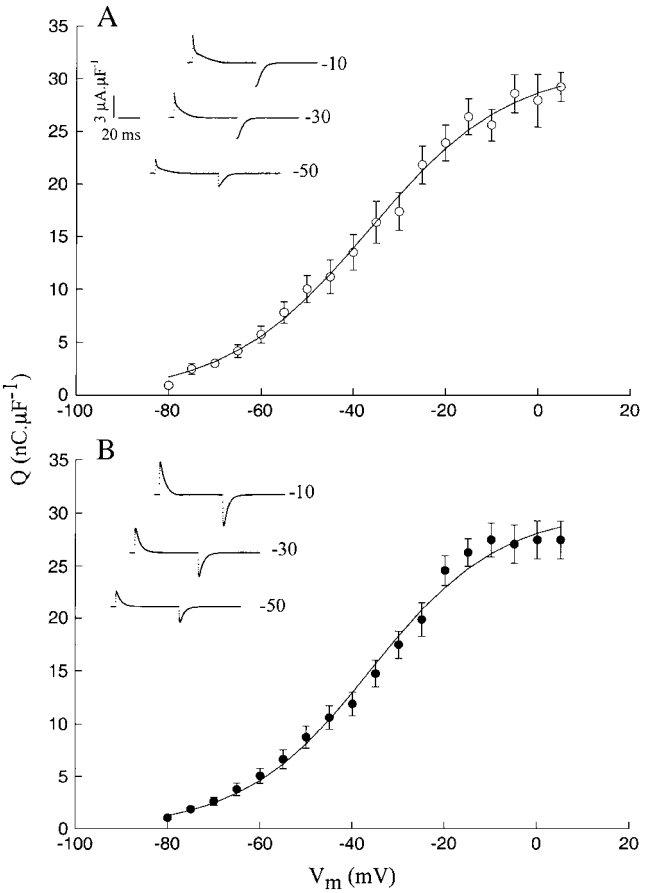

FIGURE 3 The action of the β_{1a} subunit on charge movement. (*A*) (○) Represents mean values (± SE) of charge movement as a function of membrane potential from control experiments ($n = 16$). The smooth curve is the best fit of Eq. 3 to the data points with $Q_{max} = 31.3$ nC/μF, $V = -36.6$ mV, and $k = 15.0$ mV. (*B*) (●) Represents mean values (± SE) of charge movement as a function of membrane potential in the presence of the β_{1a} subunit ($n = 16$). $E_h = -100$ mV. The smooth curve is the Boltzmann fit with $Q_{max} = 30.2$ nC/μF, $V = -36.0$ mV, and $k = 13.9$ mV. The insets in panels *A* and *B* show records of nonlinear currents from representative experiments. The amplitude and timescale in panel *A* also applies to panel *B*.

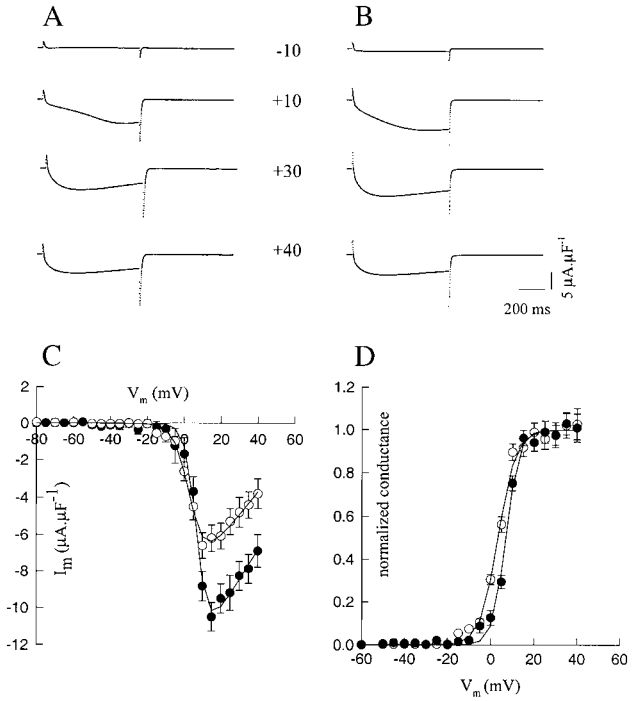

FIGURE 4 The action of the β_{1a} subunit on L-type currents. (*A*) The records show nonlinear currents from a control experiment at the potentials indicated with the numbers (in mV) between traces. (*B*) Records of membrane currents at the same potentials from a separate experiment performed in the presence of the β_{1a} subunit. Currents were normalized per unit capacitance. (*C*) The current-voltage relationship of Ca^{2+} currents. Symbols represent mean values (± SE) of peak Ca^{2+} currents from control experiments (○) ($n = 21$) and from experiments performed in the presence of the β_{1a} subunit (●) ($n = 16$). $E_h = -80$ mV. The smooth curve is the best fit of Eq. 4 to the data points with $G_{max} = 122.5$ μS/μF, $V = 3.4$ mV, $k = 4.2$ mV, and $V_{rev} = 70.2$ mV (○) and $G_{max} = 163.6$ μS/μF, $V = 7.0$ mV, $k = 3.1$ mV, and $V_{rev} = 81.7$ mV (●). (*D*) The voltage dependence of the normalized conductance. Mean current density values from panel *C* were divided by $G_{max} \times (V_m - V_{rev})$. Smooth curves are best fits of a Boltzmann function with $V = 3.4$ mV and $k = 4.1$ mV (○) and $V = 7.0$ mV and $k = 3.0$ mV (●).

with the numbers beside each trace. Fig. 3 *B* summarizes results from experiments in which the pipette contained the β_{1a} subunit. The maximum charge values and the voltage dependence of charge movement were very similar to those of the control experiments. This indicates that, in the short term, the β_{1a} subunit has no effect on charge movement.

Actions of the β_{1a} subunit on Ca^{2+} currents

The absence of β_{1a} subunit action on charge movement (demonstrated above) is not due to poor diffusion of the β_{1a} subunit through the patch pipette and into the fiber. This is shown here by demonstrating a clear action of this auxiliary subunit on L-type Ca^{2+} current in voltage clamp experiments performed in muscle fibers. We found that the β_{1a} subunit increased the amplitude of I_{Ca} (Fig. 4, *A–D*). Fig. 4 *A* illustrates control currents at the potentials indicated (in mV). The amplitude and time course of I_{Ca} depended on the membrane depolarization level. I_{Ca} was not sustained, but declined during the pulse by a voltage-dependent inactivation process. Fig. 4 *B* illustrates records from a similar experiment except for the presence of the β_{1a} subunit. The amplitude of I_{Ca} was distinctly larger at all potentials although their time course was not substantially changed. For example, the time to peak of I_{Ca} at +30 mV was 262 ms in panel *A*, and 270 ms in panel *B*. Likewise, the time to peak of I_{Ca} at large depolarizations averaged 247.2 ± 12.9 ms ($n = 21$) in control experiments and it averaged 233.0 ± 11.2 ms ($n = 16$) in the presence of the β_{1a} subunit.

Fig. 4 *C* shows the average current-voltage relationship derived from several experiments as that illustrated in Fig. 4, *A* and *B*. Open symbols represent the control experiment and solid symbols experiments in the presence of the β_{1a} subunit.

Compared to currents recorded under control conditions, currents recorded in the presence of the β_{1a} subunit were significantly larger ($p < 0.05$) at positive potentials. The smooth curves through the data points in Fig. 4 *C* represent the best fit of Eq. 4 with the parameters indicated in the legend. The most significant effect of the β_{1a} subunit on the I-V curve was to increase the values of G_{max}. There were only minor shifts along the voltage axis, as illustrated in Fig. 4 *D*, which represents the relationship between the normalized conductance and membrane potential in both experimental conditions.

Role of the carboxy-terminus on potentiation of Ca^{2+} signals

The carboxy-terminus region of the β_{1a} subunit is essential for the restoration of E-C coupling in β-null myotubes to levels similar to those of control cells (37). Therefore, the role of this region in the potentiation of Ca^{2+} transients induced by action potentials was examined. Fig. 5 *A* shows representative Ca^{2+} signals from a fiber that was pressure injected with the β_{1a} subunit purified from bacteria. Consistent with the data illustrated in Fig. 1 *B*, there was a gradual increase in the amplitude of the signals that reached a peak value 16 min after injection. After that, there was a slow return to control values. In contrast, when a truncated β_{1a} subunit (lacking 40 amino acids in the carboxy-terminus region) was pressure-injected, the amplitude of the Ca^{2+} signals remained unchanged. Similar results were observed in 15 other experiments. The peak $\Delta F/F$ values averaged 4.1 ± 0.2 ($n = 16$) before pressure injection and 3.9 ± 0.2 ($n = 16$), 20 min after the truncated form of the β_{1a} subunit was pressure injected. Likewise, electrophysiological experiments revealed that the truncated form of the β_{1a} subunit had no effect on L-type currents or on charge movement.

Peak I_{Ca} values were -6.2 ± 0.7 μA/μF ($n = 5$) in control experiments and 5.9 ± 0.7 μA/μF ($n = 6$) in the presence of truncated β-subunits. The Boltzmann parameters from charge movement experiments were: $Q_{max} = 33.5 \pm 2.3$ nC/μF, $V = -40.1 \pm 2.0$ mV, and $k = 14.6 \pm 2.1$ mV ($n = 5$) for control experiments and $Q_{max} = 32.1 \pm 3.8$ nC/μF, $V = -39.2 \pm 1.9$ mV, and $k = 15.1 \pm 2.7$ mV ($n = 7$) from experiments performed with the truncated β_{1a} protein.

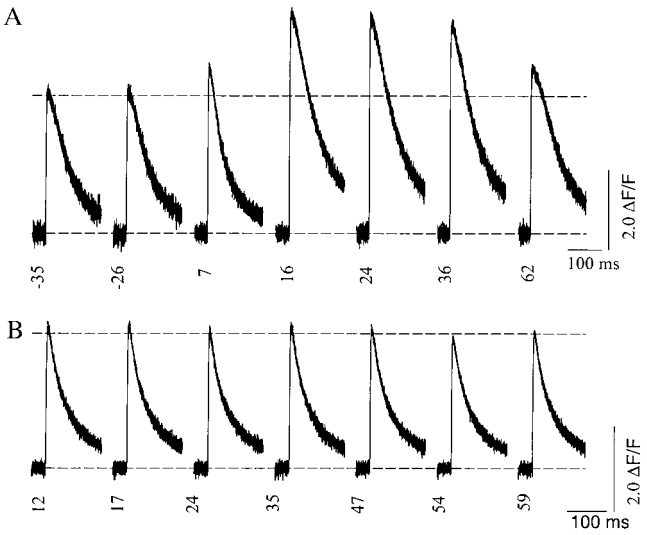

FIGURE 5 The involvement of the carboxy-terminus region of the β_{1a} subunit on Ca^{2+} signal potentiation. (*A*) The records show Fluo-3 Ca^{2+} signals associated with action potentials from a muscle fiber that was pressure injected with the full-length β_{1a} subunit purified from bacteria. (*B*) Ca^{2+} signals from a separate fiber to which a truncated form of the β_{1a} subunit, lacking 40 amino acids in the carboxy-terminus region, was pressure injected. The numbers below each trace indicate time in minutes computed since microinjection was carried out. The dotted lines indicate resting fluorescence and peak $\Delta F/F$ before pressure injection.

Action of the β_{1a} subunit on SR Ca^{2+} release channels

The possibility that the β_{1a} subunit protein is acting directly on SR Ca^{2+} release channels was tested by performing SR Ca^{2+} leak and bilayer experiments. Fig. 6 *A* shows the action of the β_{1a} subunit on RyR-mediated Ca^{2+} leak from a population of heavy SR membrane microsomes. The SR

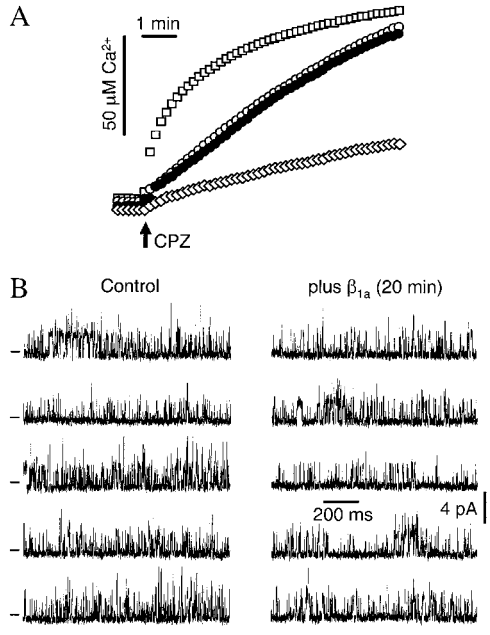

FIGURE 6 The action of the β_{1a} subunit on Ca^{2+} leak from SR microsomes and on single RyR1 channel function. (*A*) The Ca^{2+} leak rate of Ca^{2+} loaded skeletal muscle SR microsomes (50 μg) was recorded after SERCA pump blockade by 25 μM cyclopiazonic acid (*CPZ*). Leak was measured in different experimental conditions (□, 2.5 mM caffeine; ◇, 5 μM ruthenium red; ●, β_{1a} subunit; ○, truncated β_{1a} subunit). (*B*) Single RyR1 channel activity in planar lipid bilayers was monitored in the absence (*control*) and presence of the β_{1a} subunit. The charge carrier was Ca^{2+} and holding potential was 0 mV. The solution in the cytosolic chamber had 2 μM free Ca^{2+}, 5.5 mM total Mg^{2+}, and 7.0 mM total ATP.

microsome population was actively Ca^{2+} loaded using the ATP driven SERCA pump. The pump was then blocked with CPZ and the rate of Ca^{2+} leak from the microsomes measured in five different experimental conditions (control, caffeine, ruthenium red, β_{1a}, and truncated β_{1a}). Open diamonds and squares show leak rates in the presence of ruthenium red and caffeine, respectively. Ruthenium red slowed leak rate whereas caffeine accelerated the leak. The average leak rate (nM Ca mg protein^{-1}min^{-1}) was 17.7 ± 2.4 ($n = 6$) in ruthenium red and 489 ± 55 ($n = 6$) in caffeine. Open and solid circles show leak rates in the presence of the β_{1a} subunit and truncated β_{1a} subunit, respectively. The average leak rate was 64.9 ± 7.7 ($n = 6$) with the β_{1a} subunit added and 62.8 ± 8.8 ($n = 6$) when the truncated β_{1a} subunit was added. The leak rates with the normal and truncated subunits were virtually identical and overlap control leak data (i.e., leak after CPZ application without another added reagent; data not shown). This result suggests that the β_{1a} subunit does not activate RyR-mediated Ca^{2+} release from SR microsomes.

Fig. 6 *B* shows the action of the β_{1a} subunit on single RyR1 channel function. The SR microsomes used above were fused into planar lipid bilayers and RyR1 channel activity recorded. Open events are shown as upward deflections from the zero current level (marked). In most cases, multiple RyR1 channels were incorporated into the bilayers. The β_{1a} subunit was added to the cytosolic chamber in six different experiments. Representative channel recordings are shown. Addition of the β_{1a} subunit did not induce a detectable change in unit Ca^{2+} current or open probability. The average open probability (*nPo*) was 0.16 ± 0.04 ($n = 6$) in control and 0.23 ± 0.05 ($n = 6$) after the β_{1a} subunit was added. This result suggests that the β_{1a} subunit does not affect the RyR1 channel when it was directly applied to the isolated channel in a bilayer. The SR Ca^{2+} leak and single channel data (Fig. 6) combined imply that the β_{1a} subunit potentiation of the action potential induced Ca^{2+} transient in muscle fibers is not likely due to a direct action of the β_{1a} subunit on the RyR1 channel.

DISCUSSION

Role of the β-subunit on Ca^{2+} release

The major finding of this study is that the acute application of β_{1a} subunits increases the amount of Ca^{2+} that is released by an action potential. Although the underlying mechanism of the potentiation of Ca^{2+} signals by β_{1a} subunits is unknown, the fact that no changes in charge movement were observed suggests that the β_{1a} subunit improves the efficiency of the coupling mechanism, where the same number of voltage sensors would open more Ca^{2+} release channels. Alternatively, the β_{1a} subunit may improve the effectiveness of the Ca^{2+}-induced Ca^{2+} release mechanism that is known to operate in skeletal muscle, although Ca^{2+}-induced Ca^{2+} release is a minor component in mammalian skeletal muscle (38) and no direct action of the β_{1a} subunit on the RyR1 channel was detected in our studies.

An alternative explanation would involve binding of the β_{1a} subunit to intracellular factors that regulate Ca^{2+} release. The SR Ca release process is regulated by numerous factors in cells. The presence of some of these factors (e.g., sorcin) may chronically inhibit the SR Ca^{2+} release process. If these chronically inhibitory factors also interact with the β_{1a} subunit, the application of excess β_{1a} subunits could alter the way this factor regulates release. The addition of excess β_{1a} protein could hypothetically result in larger Ca^{2+} release simply by interacting with this factor. Based on the current absence of data supporting this alternative interpretation, we believe an increase in coupling efficiency is more likely the underlying mechanism involved.

From a structural point of view, potentiation of Ca^{2+} signals could be explained in two ways. The first possibility is that not all α_{1s} subunits in the transverse tubular system (TTS) membranes are associated with β_{1a} subunits. In this scenario, the exogenously added β_{1a} subunit would bind to free α_{1s} subunits to exert their action. However, this is very unlikely because the β_{1a} subunit is essential for the targeting of the channel (12) and thus all correctly targeted α_{1s} subunits should have associated β_{1a} subunits. As discussed by Dolphin (39), however, it is possible that the affinity of α_{1s} subunits for β_{1a} subunits is reduced once the channel has reached the TTS membranes. The second possibility is that there are multiple binding sites between α_{1s} and β_{1a} subunits (40). In this scenario, additional β_{1a} subunits would bind to a single α_{1s} subunit modulating the interaction between the α_{1s} subunit and the RyR1 channel. In either case, the β_{1a} subunit would modulate the signal transduction process involved in EC coupling.

Role of the C-terminus region

Our data further indicate that the carboxy-terminus region of the β_{1a} subunit is essential for potentiation of Ca^{2+} transients. Previous work has established that this region is required for restoration of normal E-C coupling in β-null cells (37,41) and it is different from the high affinity site in β (the BID region), a 30-amino-acid N-terminal region of its second conserved domain (42), that interacts with a high-affinity site in the α-subunit (the AID region) (43,44). It is thus possible that higher order regulatory complexes are formed where the β_{1a} subunit binds to the α_{1s} subunit in different regions. The high-affinity binding site would provide the structural basis for the strong interaction between α_{1s} and β_{1a} subunits allowing the trafficking and expression of α_{1s} in TTS. The regulatory effects of the β_{1a} subunit on Ca^{2+} release that we report here, might result from the interaction of $\alpha_{1s}\beta_{1a}$ complexes with a second β_{1a} subunit, possibly mediated by low-affinity sites. This last possibility is fully compatible with these findings, since the time course of the effect of the β_{1a} subunit on Ca^{2+} signals could be

described by a purely diffusional process. The additional interaction of a β_{1a} subunit with the $Ca_V1.1$ channel would not necessarily lead to the formation of a stable complex as it has been described for the β-modulation of the α_{1c} channel (45). Also, low-affinity sites in the α_1 subunit of Ca^{2+} channels have been described in regions distant from the AID region (46,44,47,48), and based on the effects of increasing concentrations of β_3 on α_{1A} subunit, it has been suggested that there are two distinct binding processes for β-subunits (49). A low-affinity interaction between α_{1s} and β_{1a} subunits would be more easily switched ''on'' and ''off'' as expected from a regulatory process.

Is the α_{1s} subunit function limited by the β-subunit?

These results suggest a different role of β-subunits from the classical action on trafficking of the channels to the plasma membrane. The capability of the β_{1a} subunit to potentiate Ca^{2+} transients in the short term, suggests that this auxiliary subunit is a limiting factor regulating the amount of Ca^{2+} that is released by the SR. Therefore, the α_1 subunits of skeletal muscle are not normally saturated with β, raising the possibility that Ca release may be regulated by β-subunits under physiological conditions. In this regard, there are several previous observations suggesting that the function of α_1 subunits is limited by the amount of β-subunits available. Thus, when $Ca_V1.1$ channels in a cell-free preparation are exposed to additional β_{1a} subunits, a potentiation of L-type Ca^{2+} channel currents is observed (15). Also, overexpression of β-subunits in adult heart cells increases whole-cell, L-type Ca^{2+} currents, and maximal gating charge (48), whereas overexpression of α_{1c} in a transgenic mouse model does not lead to increases in Ca^{2+} channel current density values (50). The observations of Yamaguchi et al. (51) are also consistent with the idea that the concentration of β-subunits is limiting: the injection of β_3 subunit protein increases $Ca_V1.2$ currents in *Xenopus* oocytes and it has acute effects on the biophysical properties of the channel.

A physiological modulation of Ca release by β-subunits would not be expected to involve a very high concentration of these proteins. In this regard, we used in these experiments an amount of β-protein that is distinctly lower (at least five times) than the one used in the experiments of Yamaguchi et al. (51) and Opatowsky et al. (52). A physiological role of the β-subunits on Ca release in muscle would require the presence of an intracellular pool of β-proteins that could be shuttled to the membrane where they would bind to α_1 subunits leading to changes in the interaction between α_1 subunits and RyR1. The presence of β-subunits in skeletal muscle, not associated with α_1 subunits, has indeed been described in tissue homogenates (53).

We thank Dr. Roberto Coronado and Dr. Zurisaddai Hernández for relevant discussions and advice, Dr. Patricia Powers for the β_{1a} cDNA, and Dr. Julio Vergara for providing the pressure injection system. We thank Rodrigo Sanchez for data analysis. We also thank Oscar Ramírez, Rubén García, Maura Porta, and Dr. Paula Diaz-Sylvester for technical assistance and Ms. Susana Zamudio for secretarial work.

This work was supported by CONACyT grants, 41180-N and 37356-N, and by National Institutes of Health grants R01 HL63903 and HL57832, MDA3699.

REFERENCES

1. Ríos, E., and G. Pizarro. 1991. Voltage sensor of excitation-contraction coupling in skeletal muscle. *Physiol. Rev.* 71:849–908.
2. Lamb, G. D. 1992. DHP receptors and excitation-contraction coupling. *J. Muscle Res. Cell Motil.* 13:394–405.
3. Huang, C. L. H. 1993. Intramembrane Charge Movements in Striated Muscle. Clarendon Press, Oxford, UK.
4. Melzer, W., A. Herrmann-Frank, and H. C. Luttgau. 1995. The role of Ca^{2+} ions in excitation-contraction coupling of skeletal muscle fibres. *Biochim. Biophys. Acta.* 1241:59–116.
5. Sánchez, J. A., and E. Stefani. 1983. Kinetic properties of calcium channels of twitch muscle fibres of the frog. *J. Physiol.* 337:1–17.
6. Ertel, E. A., K. P. Campbell, M. M. Harpold, F. Hofmann, Y. Mori, E. Perez-Reyes, A. Schwartz, T. P. Snutch, T. Tanabe, L. Birnbaumer, R. W. Tsien, and W. A. Catterall. 2000. Nomenclature of voltage-gated calcium channels. *Neuron.* 25:533–535.
7. Perez-Reyes, E., H. S. Klim, A. Lacerda, W. Horne, X. Wei, D. Rampe, K. P. Campbell, A. M. Brown, and L. Birnbaumer. 1989. Induction of calcium currents by the expression of the β1-subunit of the dihydropyridine receptor from skeletal muscle. *Nature.* 340:233–236.
8. Hofmann, F., M. Biel, and V. Flockerzi. 1994. Molecular basis for Ca^{2+} channel diversity. *Annu. Rev. Neurosci.* 17:399–418.
9. Isom, L. L., J. S. De Jongh, and W. Catterall. 1994. Auxiliary subunits of voltage gated ion channels. *Neuron.* 12:1183–1194.
10. Catterall, W. A. 2000. Structure and regulation of voltage-gated Ca^{2+} channels. *Annu. Rev. Cell Dev. Biol.* 16:521–555.
11. Ren, D., and L. M. Hall. 1997. Functional expression and characterization of skeletal muscle dihydropyridine receptors in Xenopus oocytes. *J. Biol. Chem.* 272:22393–22396.
12. Gregg, R. G., A. Messing, C. Strube, M. Beurg, R. Moss, M. Behan, M. Sukhareva, S. Haynes, J. A. Powell, R. Coronado, and P. A. Powers. 1996. Absence of the β subunit (*cchb1*) of the skeletal muscle dihydropyridine receptor alters expression of the α_1 subunit and eliminates excitation-contraction coupling. *Proc. Natl. Acad. Sci. USA.* 93:13961–13966.
13. Beurg, M., M. Sukhareva, C. A. Ahern, M. W. Conklin, E. Perez-Reyes, P. A. Powers, R. G. Gregg, and R. Coronado. 1999. Differential regulation of skeletal muscle L-type Ca^{2+} current and excitation-contraction coupling by the dihydropyridine receptor β_1 subunit. *Biophys. J.* 76:1744–1756.
14. Beurg, M., M. Sukhareva, C. Strube, P. A. Powers, R. G. Gregg, and R. Coronado. 1997. Recovery of Ca^{2+} current, charge movements, and Ca^{2+} transients in myotubes deficient in dihydropyridine receptor β_1 subunit transfected with β_1 cDNA. *Biophys. J.* 73:807–818.
15. García, R., E. Carrillo, S. Rebolledo, M. C. García, and J. A. Sánchez. 2002. The β_{1a} subunit regulates the functional properties of adult frog and mouse L-type Ca^{2+} channels of skeletal muscle. *J. Physiol.* 545:407–419.
16. García, M. C., R. García, E. Carrillo, and J. A. Sánchez. 2004. The β_{1a} subunit enhances the amplitude of L-type Ca^{2+} currents and Ca^{2+} signals of adult mouse skeletal muscle fibers. *Biophys. J.* 86:63A (Abstr.).
17. Smith, A. J. 1992. Electrophoretic separation of proteins. *In* Short Protocols in Molecular Biology. F. M. Ausubel, editor. John Wiley & Sons, NY. 1023–1026.
18. Bogdanov, Y., N. L. Brice, C. Canti, K. M. Page, M. Li, S. G. Volsen, and A. C. Dolphin. 2000. Acidic motif responsible for plasma

membrane association of the voltage-dependent calcium channel β_{1b} subunit. *Eur. J. Neurosci.* 12:894–902.

19. Hanlon, M. R., N. S. Berrow, A. C. Dolphin, and B. A. Wallace. 1999. Modelling of a voltage-dependent Ca^{2+} channel β subunit as a basis for understanding its functional properties. *FEBS Lett.* 445:366–370.
20. Richards, M. W., A. J. Butcher, and A. C. Dolphin. 2004. Ca^{2+} channel β-subunits: structural insights AID our understanding. *Trends Pharmacol. Sci.* 25:626–632.
21. Sheridan, D. C., W. Cheng, L. Carbonneau, C. A. Ahern, and R. Coronado. 2004. Involvement of a heptad repeat in the carboxyl terminus of the dihydropiridine receptor β_{1a} subunit in the mechanism of excitation-contraction coupling in skeletal muscle. *Biophys. J.* 87: 929–942.
22. Papadopoulos, S., K. D. Jurgens, and G. Gros. 2000. Protein diffusion in living skeletal muscle fibers: dependence on protein size, fiber type, and contraction. *Biophys. J.* 79:2084–2094.
23. Thomas, D., S. C. Tovey, T. J. Collins, M. D. Bootman, M. J. Berridge, and P. Lipp. 2000. A comparison of fluorescent Ca^{2+} indicator properties and their use in measuring elementary and global Ca^{2+} signals. *Cell Calcium.* 28:213–233.
24. Vergara, J., M. Difranco, D. Compagnon, and B. Suárez-Isla. 1991. Imaging of calcium transients in skeletal muscle fibers. *Biophys. J.* 59:12–24.
25. Caputo, C., and P. Bolaños. 1994. Fluo-3 signals associated with potassium contractures in single amphibian muscle fibres. *J. Physiol.* 481:119–128.
26. Lacampagne, A., M. G. Klein, C. W. Ward, and M. F. Schneider. 2000. Two mechanisms for termination of individual Ca^{2+} sparks in skeletal muscle. *Proc. Natl. Acad. Sci. USA.* 97:7823–7828.
27. Shirokova, N., J. García, and E. Rios. 1998. Local calcium release in mammalian skeletal muscle. *J. Physiol.* 512:377–384.
28. Carroll, S. L., M. G. Klein, and M. F. Schneider. 1995. Calcium transients in intact rat skeletal muscle fibers in agarose gel. *Am. J. Physiol.* 269:C28–C34.
29. Saito, A., S. Seiler, A. Chu, and S. Fleischer. 1984. Preparation and morphology of sarcoplasmic reticulum terminal cisternae from rabbit skeletal muscle. *J. Cell Biol.* 99:875–885.
30. Copello, J. A., Y. Qi, L. H. Jeyakumar, E. Ogunbunmi, and S. Fleischer. 2001. Lack of effect of cADP-ribose and NAADP on the activity of skeletal muscle and heart ryanodine receptors. *Cell Calcium.* 30:269–284.
31. Hamill, O. P., A. Marty, E. Neher, B. Sakmann, and F. J. Sigworth. 1981. Improved patch-clamp techniques for high-resolution current recording from cells and cell-free membrane patches. *Pflugers Arch.* 391:85–100.
32. Wang, Z., M. L. Messie, and O. Delbono. 1999. Patch-clamp recording of charge movement, Ca^{2+} current, and Ca^{2+} transients in adult skeletal muscle fibers. *Biophys. J.* 77:2709–2716.
33. Copello, J. A., S. Barg, A. Sonnleitner, M. Porta, P. Diaz-Sylvester, M. Fill, H. Schindler, and S. Fleischer. 2002. Differential activation by Ca^{2+}, ATP and caffeine of cardiac and skeletal muscle ryanodine receptors after block by Mg^{2+}. *J. Membr. Biol.* 187:51–64.
34. Francini, F., C. Bencini, C. Piperio, and R. Squecco. 2001. Separation of charge movement components in mammalian skeletal muscle fibres. *J. Physiol.* 537:45–56.
35. Horowicz, P., and M. F. Schneider. 1981. Membrane charge movement in contracting and non-contracting skeletal muscle fibres. *J. Physiol.* 314:565–593.
36. Collet, C., L. Csernoch, and V. Jacquemond. 2003. Intramembrane charge movement and L-type calcium current in skeletal muscle fibers isolated from control and *mdx* mice. *Biophys. J.* 84:251–265.
37. Beurg, M., C. A. Ahern, P. Vallejo, M. W. Conklin, P. A. Powers, R. G. Gregg, and R. Coronado. 1999. Involvement of the carboxy-terminus region of the dihydropyridine receptor β_{1a} subunit in excitation-contraction coupling of skeletal muscle. *Biophys. J.* 77:2953–2967.
38. Murayama, T., and Y. Ogawa. 2002. Roles of two ryanodine receptor isoforms coexisting in skeletal muscle. *Trends Cardiovasc. Med.* 12: 305–311.
39. Dolphin, A. C. 2003. β subunits of voltage-gated calcium channels. *J. Bioenerg. Biomembr.* 35:599–619.
40. Jones, S. W. 2002. Calcium channels: when is a subunit not a subunit? *J. Physiol.* 545:334.
41. Sheridan, D. C., W. Cheng, C. A. Ahern, L. Mortenson, D. Alsammarae, P. Vallejo, and R. Coronado. 2003. Truncation of the carboxyl terminus of the dihydropyridine receptor β_{1a} subunit promotes Ca^{2+} dependent excitation-contraction coupling in skeletal myotubes. *Biophys. J.* 84:220–237.
42. De Waard, M., M. Pragnell, and K. P. Campbell. 1994. Ca^{2+} channel regulation by a conserved beta subunit domain. *Neuron.* 13:495–503.
43. Pragnell, M., M. De Waard, Y. Mori, T. Tanabe, T. P. Snutch, and K. P. Campbell. 1994. Calcium channel β subunit binds to a conserved motif in the I–II cytoplasmic linker of the α_1-subunit. *Nature.* 368: 67–70.
44. Walker, D., and M. De Waard. 1998. Subunit interaction sites in voltage-dependent Ca^{2+} channels: role in channel function. *Trends Neurosci.* 21:148–154.
45. Gerster, U., B. Neuhuber, K. Groschner, J. Striessnig, and B. E. Flucher. 1999. Current modulation and membrane targeting of the calcium channel α_{1C} subunit are independent functions of the β subunit. *J. Physiol.* 517:353–368.
46. Qin, N., D. Platano, R. Olcese, E. Stefani, and L. Birnbaumer. 1997. Direct interaction of $G\beta\gamma$ with a C-terminal $G\beta\gamma$-binding domain of the Ca^{2+} channel α_1 subunit is responsible for channel inhibition by G protein-coupled receptors. *Proc. Natl. Acad. Sci. USA.* 94:8866–8871.
47. Walker, D., D. Bichet, S. Geib, E. Mori, V. Cornet, T. P. Snutch, Y. Mori, and M. De Waard. 1999. A new β subtype-specific interaction in α_{1A} subunit controls P/Q-type Ca^{2+} channel activation. *J. Biol. Chem.* 274:12383–12390.
48. Colecraft, H. M., B. Alseikhan, S. X. Takahashi, D. Chaudhuri, S. Mittman, V. Yegnasubramanian, R. S. Alvania, D. C. Johns, E. Marban, and D. T. Yue. 2002. Novel functional properties of Ca^{2+} channel beta subunits revealed by their expression in adult rat heart cells. *J. Physiol.* 541:435–452.
49. Canti, C., A. Davies, N. S. Berrow, A. J. Butcher, K. M. Page, and A. C. Dolphin. 2001. Evidence for two concentration-dependent processes for β-subunit effects on α_{1B} calcium channels. *Biophys. J.* 81: 1439–1451.
50. Muth, J. N., H. Yamaguchi, G. Mikala, I. L. Grupp, W. Lewis, H. Cheng, L. S. Song, E. G. Lakatta, G. Varadi, and A. Schwartz. 1999. Cardiac-specific overexpression of the α_1 subunit of the L-type voltage-dependent Ca^{2+} channel in transgenic mice. Loss of isoproterenol-induced contraction. *J. Biol. Chem.* 274:21503–21506.
51. Yamaguchi, H., M. Hara, M. Strobeck, K. Fukasawa, A. Schwartz, and G. Varadi. 1998. Multiple modulation pathways of calcium channel activity by a β subunit. *J. Biol. Chem.* 273:19348–19356.
52. Optatowsky, Y., O. Chomsky-Hecht, K. Myoung-Goo, K. P. Campbell, and J. A. Hirsch. 2003. The voltage-dependent calcium channel β subunit contains two stable interacting domains. *J. Biol. Chem.* 278: 52323–52332.
53. Witcher, D. R., M. De Waard, H. Liu, M. Pragnell, and K. P. Campbell. 1995. Association of native Ca^{2+} channel β subunits with the α_1 subunit interaction domain. *J. Biol. Chem.* 270:18088–18093.